

Anisotropy of magnetic susceptibility of earthquake-affected soft sediments: example from Ther village, Latur, Maharashtra, India

B. V. Lakshmi*, K. V. V. Satyanarayana, N. Basavaiah and Praveen Gawali

Indian Institute of Geomagnetism, Kalamboli Highway, New Panvel (W), Navi Mumbai 410 218, India

Anisotropy of magnetic susceptibility (AMS) of deformed and undeformed unconsolidated clay samples of Deccan Trap terrain from the ~2000-year-old palaeo-earthquake site of Ther village, Maharashtra, India, was studied. Such deposits are rare in this region and give an exceptional opportunity to test the efficacy of AMS and other magneto petrofabric studies, which can have a bearing on magnetic granularity ellipsoids, inclination and declination directions impacting palaeomagnetic studies. The undeformed clay samples exhibit typical sedimentary fabric with an oblate AMS ellipsoid, whereas the deformed samples are tightly grouped in the inferred compression direction, probably effected by an earthquake, exhibiting prolate as well as oblate AMS ellipsoids. The temperature-dependent magnetic susceptibility revealed the occurrence of titanomagnetite and magnetite in both the deformed and undeformed samples signifying similar sediment material. The site mean ChRM direction for undeformed clay samples is $D = 3$ and $I = 44.7$ ($k = 92.7$, $\alpha_{95} = 4.5$), whereas for deformed samples $D = 336$ and $I = 39$ ($k = 39$, $\alpha_{95} = 8$). The present study reveals that sediments can be severely deformed without deflecting minimum susceptibility directions. AMS methodology can be effective in the DT region and can throw up new results to build the chronology of past earthquakes.

Keywords: Anisotropy of magnetic susceptibility, characteristic remanent magnetization, earthquake, soft sediments.

EARTHQUAKE-related hazards, e.g. major large-scale faulting and fracturing, shaking, tsunami, earth slides, mud flows, soft-sediment deformation structures, sediment liquefaction, etc. have posed great threat to humanity and its ambient environment. Soft-sediment deformation structures related to earthquakes (i.e. seismites) are important diagnostic features in palaeoseismology¹⁻⁷. Recently, various workers have reported seismically induced soft-sediment deformation structures in the seismically active regions of India⁸⁻¹⁴. However, very little published documentation exists on soft-sedimentary deformations generated by seismic shocks that affect soils in the

Deccan Trap (DT) region. The characterization at such shallow levels is important in determining regional seismicity and syn-sedimentary tectonic activity in depositional settings that are commonly characterized by tectonic quiescence.

The Killari earthquake of 30 September 1993 attracted attention to the damaging effects of an earthquake, even in stable cratonic setting such as the DT terrain. This area was considered aseismic for a long time; following the September 1993 earthquake, scientists are trying to find the periodicity and repeatability of seismic events in this region. Sukhija *et al.*¹⁵ identified a large palaeoseismic event about 2000-yrs-old along Tirna River at Ther. Babar *et al.*¹⁶ have placed palaeoseismic activity along the Tirna valley from AD 971 to 1183 and around AD 1151 to 353. Rajendran¹⁷ reported evidence for at least one ancient earthquake around AD 450 at Ther. Such studies have been carried out in shield regions of Australia and North America^{18,19}, which suggested recurrence interval of 10,000–100,000 years or more for the stable interior of continents.

Similar studies are, however, difficult in the Deccan Trap terrain because unconsolidated sedimentary successions are too few and scattered in this region.

In the present communication, we report preliminary magnetic observations on the seismically induced deformations of argillaceous sediments from Ther village, which was produced by the Latur earthquake about 2000 years ago.

The deformational features developed in the sedimentary sections at Ther village (Figure 1a). This palaeoearthquake was identified by deformation features in a ~9 m thick unconsolidated sequence of clay bed (Figure 1b). The deformation structures exposed in the studied sedimentary section include flexures, warps and vertical offsets. The main deformational feature is the vertical offset of some marker horizons in the section that indicates a displacement of sedimentary beds by ~15–25 cm (Figure 1b and c) and regional compressive stresses acting in the northeast–southwest direction¹⁷. On top of this sequence lies a thick artificial dump (disaggregated basalt), which is totally undisturbed.

The west to east-flowing Tirna River drains through a part of the Ther village, and several alluvial mounds covering a few square kilometres in this area occur along both sides of the river (Figure 1a). The village is spread over these irregular and highly dissected mounds. Alternating unconsolidated layers of coarse sand with cobble deposited by surges in Tirna River and silty clay in these dissected alluvial mounds are observed²⁰.

Two sites were sampled within and above the deformed clay at each site. Twelve samples from each site were collected by horizontally pushing 8 cm³ perspex bottles into the sediment. The geologic context of the sampling sites is shown in Figure 1b. Site 1 is located in the undeformed thin clay layer and site 2 is located within

*For correspondence. (e-mail: bvlakshmi@iigs.iigm.res.in)

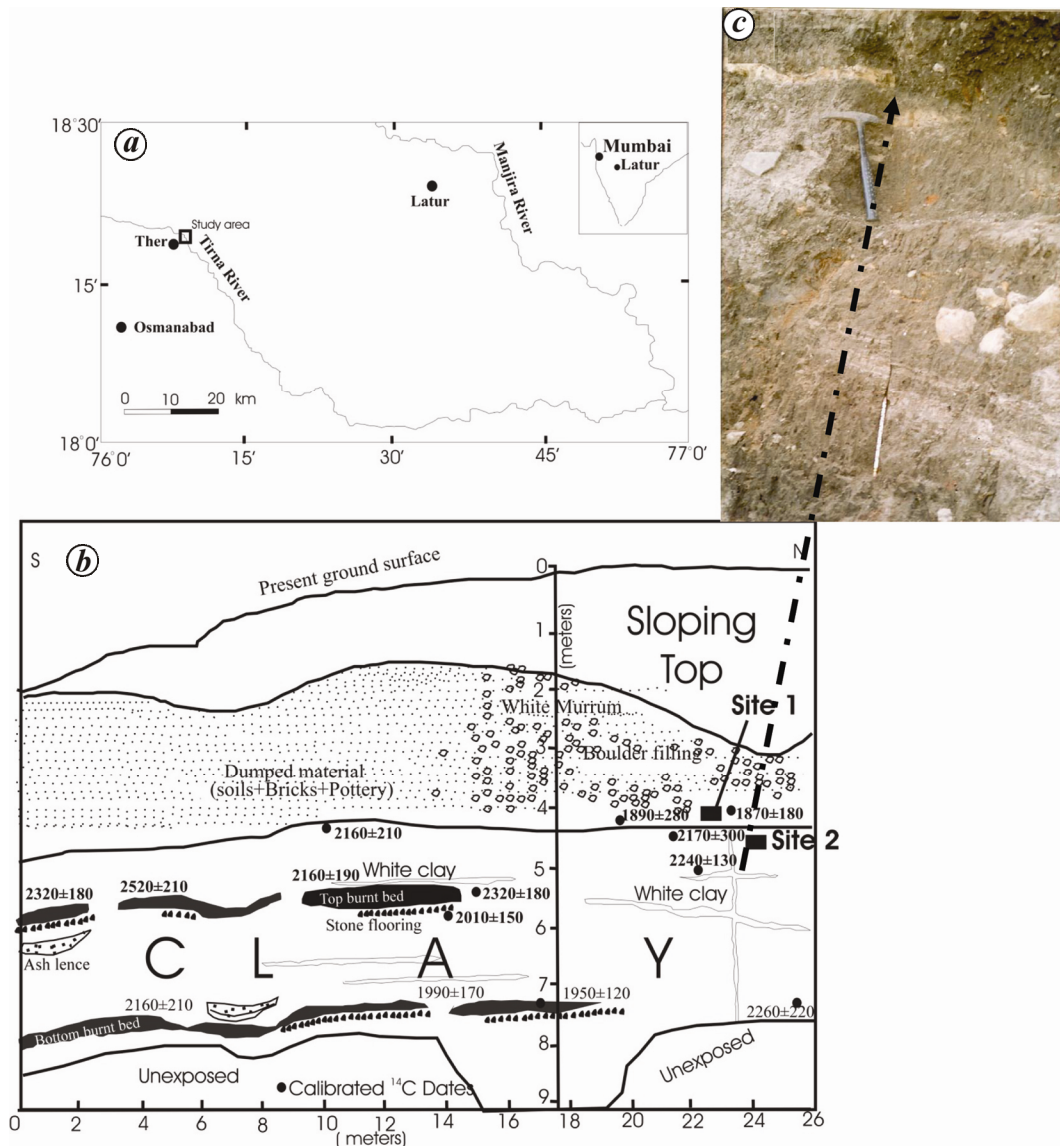


Figure 1. *a*, Location map of the study area in the Tirna River valley, Latur, Deccan Plateau, Central India (modified after Sukhija *et al.*¹⁵). *b*, Geological section along Tirna River at Ther village. The 9-m thick alluvial cross-section depicts various strata, including two burnt beds and a normal fault with a strata displacement of 15–25 cm. The fault is terminated by a thin undisturbed clay layer. The solid circles with numbers are the sampling locations for ¹⁴C dating. The calibrated dates of the organic samples are mentioned besides the sampling position. The top 4 m thick overburden is indicative of post-seismic anthropogenic build-up. Site 1 samples from the top of the undeformed clay layer, and site 2 samples from the bottom are collected from the seismically deformed clay layer for anisotropy of magnetic susceptibility (AMS) study. *c*, A clear view of vertical offset with a displacement of about 15–25 cm.

the deformed clay bed. The N–S orientation mark was drawn on the sample bottle. The bottles were sealed tightly so that *in situ* arrangement of the sediment particles was not disturbed.

All magnetic measurements were carried at the Indian Institute of Geomagnetism, Navi Mumbai, India. The anisotropy of magnetic susceptibility (AMS) was measured on a Kappabridge KLY-4S using the 15 measurement scheme of Jelinek²¹. The azimuths and magnitudes of principal susceptibility axes (K_1 , K_2 and K_3) were calculated using SUFAR software supplied by AGICO,

together with other magnetic anisotropy parameters such as anisotropy ratios, expressed as degree of anisotropy (P), shape (T) and mean susceptibility (K_m). Natural remanent magnetization (NRM) measurements of samples were made using JR-6 dual spinner magnetometer. Both alternate field (AF) and thermal demagnetization techniques were applied using ASC scientific tech AF demagnetizer and MMTD thermal demagnetizer on 24 samples from the two sites. These samples were subjected to stepwise AF demagnetization (2.5–100 mT) and thermal demagnetization (80–700°C) to remove low coercivity or

low unblocking temperature component. In all these samples, the principal components which were directed towards the origin were considered as the characteristic remanent magnetization (ChRM). ChRM was isolated by means of principal component analysis²², from at least four consecutive cleaning states at fields higher than 30 mT or temperatures higher than 350°C. Rock magnetic measurements of isothermal remanent magnetization (IRM) acquisition and backfield curves for site 1 and site 2 were performed on representative samples in steps from 10 to 1000 mT and back field application to the saturation IRM (SIRM). Remanent coercive force (Hcr) characteristic was obtained using a MMPM9 pulse magnetizer and a Molspin spinner magnetometer. Temperature dependence (40–700°C) of magnetic susceptibility (χ - T curves) was measured using KLY-4 Kappabridge.

The low-field AMS, a second-rank symmetric tensor, can be expressed in terms of three principal susceptibility axes-maximum (K_1), intermediate (K_2) and minimum (K_3)²³. In undeformed sedimentary rocks, AMS is observed with well-grouped vertical K_3 direction and dispersed K_1 and K_2 directions within a horizontal plane characterized by an oblate AMS ellipsoid^{24,25}. In moderate currents, grain imbrications in slightly off-vertical K_3 directions and K_1 directions (in lower-hemisphere projection) are antiparallel in the flow direction. In high-energy

currents with particles entrained, K_1 directions are perpendicular to the flow direction, and K_3 directions are commonly streaked, resulting in prolate or triaxial AMS ellipsoids.

The results of AMS fabric of the two sites are presented in stereographic projections in Figure 2. For undeformed bed (site 1), the K_3 axes are grouped near the vertical axis (normal to the bedding plane), while the K_1 and K_2 axes have rather scattered orientations in the bedding plane. This shows that the fabric is typically sedimentary and exhibits an oblate-shaped AMS ellipsoid (Figure 2a). The variation in degree of anisotropy (P) versus mean susceptibility (K_m), and P versus T (shape parameter) of the studied sediment samples are plotted in Figure 2c-f. Site-1 sediments are characterized by two clusters. The first one is for K_m between 3.5 and 5.1 against P ($=K_1/K_3$) ranging between 1 and 1.1 (Figure 2c), and the second is for higher range of P , between ~1.1 and 1.3, with K_m values of the samples between 1.4 and 3.8 (Figure 2c). The site-1 sediments are plotted within the oblate field in P versus T plot (Figure 2e).

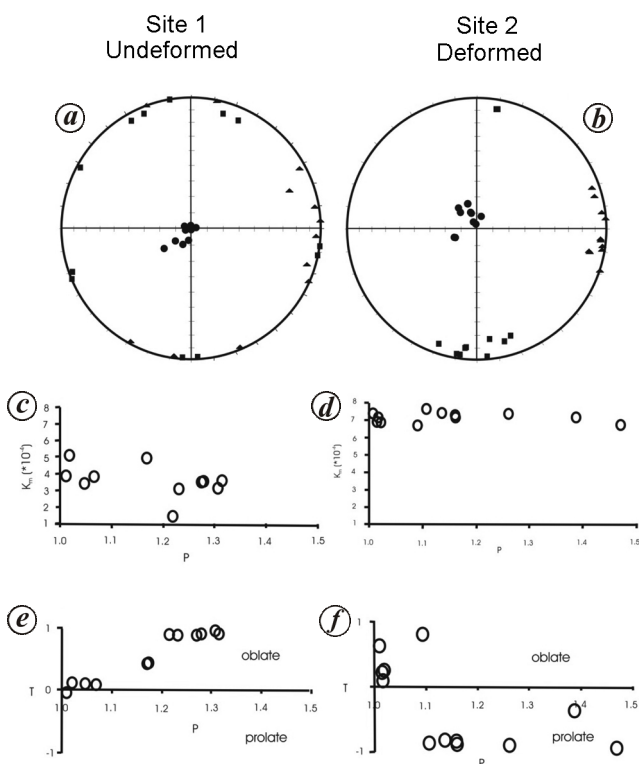


Figure 2. AMS data for two sites. *a, b*, Lower-hemisphere, equal area projections of AMS principal axes (squares: K_1 , triangles: K_2 and circles: K_3). *c, d*, Degree of anisotropy (P) versus mean susceptibility (K_m). *e, f*, P versus shape parameter (T).

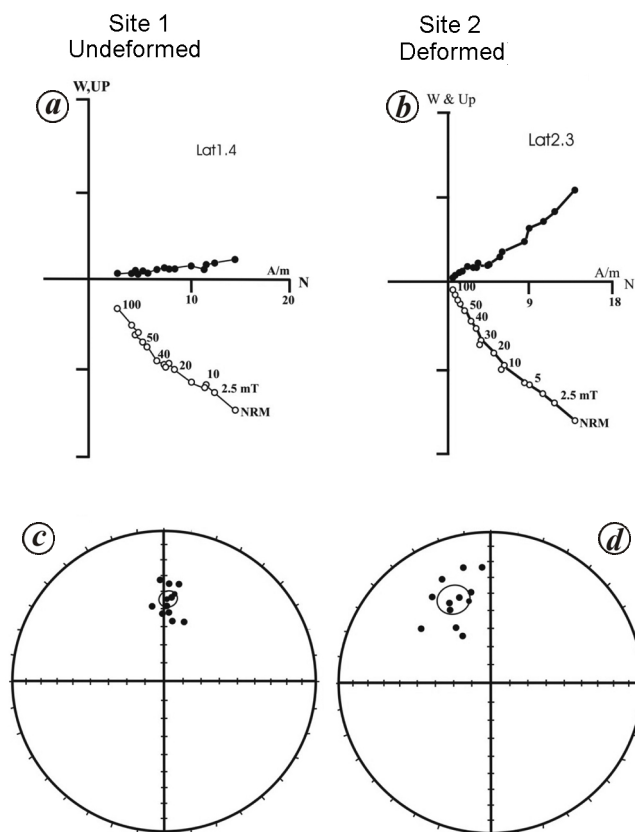


Figure 3. *a, b*, Orthogonal vector plots of alternating field demagnetization of representative samples for the two sites. Solid and open circles are horizontal and vertical projections of remanent magnetization vectors at various steps of demagnetization respectively. *c, d*, Lower-hemisphere, equal area projection of mean characteristic directions of the two sites. Solid (open) circles are projections on the lower (upper) hemisphere.

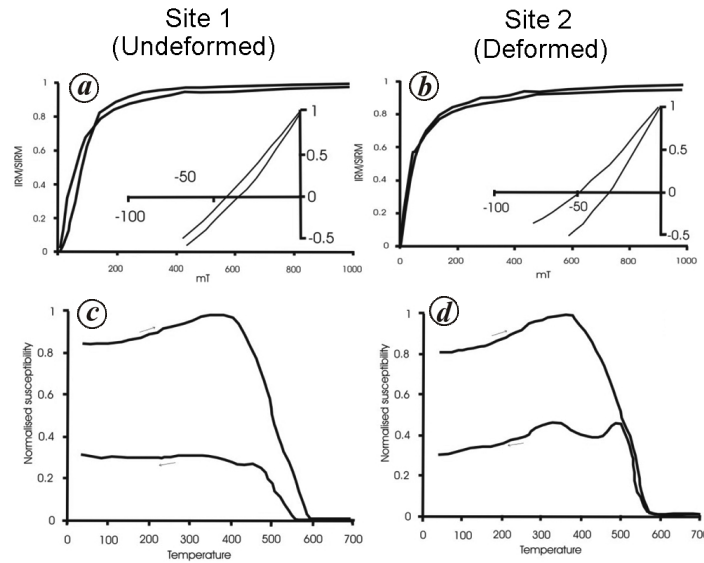


Figure 4. *a, b*, Acquisition of isothermal remanent magnetization and backfield demagnetization. *c, d*, Thermomagnetic curves for representative samples from the two sites.

Table 1. Summary of remanent magnetization directions

Site no.	No. of samples	Remanent magnetic direction			
		<i>D</i>	<i>I</i>	<i>k</i>	α_{95}
1	12	3.0	44.7	92.7	4.5
2	12	336	39	39.8	8

D, I, Mean declination and inclination; *k*, Precision parameter and α_{95} , Radius of circle of 95% confidence.

The K_3 axes from deformed bed (site 2, Figure 2 *b*) are well grouped around the vertical axis of projection and K_1 and K_2 directions are also tightly grouped into two orthogonal directions. K_1 is oriented $\sim 45^\circ$ to the direction of inferred compression (NE–SW), from the horizontal shortening revealed in the sedimentary layers. For site 2, the fabric appears in a triaxial shape. The deformed sediments are characterized by high K_m (6.8–7.8) and high P (1–1.5) values (Figure 2 *d*). For deformed sediments, the P versus T plot shows a subordinate group in the prolate field along with oblate field (Figure 2 *f*).

Comparison of the average inclinations and dispersions of K_3 axes from deformed and undeformed sediments provides a tool to identify the deformation. Several authors have devised tests for sediment deformation based on AMS fabric^{26–29}. Rosenbaum *et al.*²⁷ found that for undisturbed sections, σK_3 was 6.5° and IK_3 was 84° , while for deformed section, σK_3 was 26° and IK_3 was 66.5° . Schwehr and Tauxe²⁶ calculated σK_3 to be 18.3° and IK_3 to be 72° for the undisturbed site; for the disturbed site σK_3 was 5° and IK_3 was 80.9° . The present study obtained strikingly similar results to those by Schwehr and Tauxe²⁶. For the undeformed site, σK_3 was 6° and IK_3 is 77.6° , whereas for the deformed site σK_3 was 5° and IK_3 was 85.4° in the present study.

Typical examples of end-point vector diagrams for AF demagnetization are shown in Figure 3 *a* and *b*. The vector projections of representative samples indicate a well-defined component of ChRM by a linear decay towards the origin. These components were removed by AF fields of 2.5–25 mT (Figure 3 *a* and *b*). The direction of ChRM was determined from orthogonal plots in at least five successive measurement steps between 30 and 80 mT using principal component analysis (Figure 3). For all the studied samples, for the undeformed site, the mean ChRM directions have a mean normal polarity (Figure 3 *a*) with declination (D) = 3 and inclination (I) = 44.7 (k = 92.7, α_{95} = 4.5). For the deformed site (Figure 3 *b*), D = 336, I = 39 (k = 39, α_{95} = 8). The average NRM directions are summarized in Table 1. The deformation effect on the remanent magnetic direction had been recognized in experimental results of synthetic magnetite-bearing sandstones³⁰ and also from soft-sediment deformation resulting in scattered directions²⁶. However, as suggested by Rosenbaum *et al.*²⁷ and Cronin *et al.*³¹, it appears that even minor amounts of soft-sediment deformation can have a profound effect on the palaeomagnetic record. The present case is regarded as an example that remanent magnetization is locally affected by the sediment deformation.

Measurements of IRM, backfield curves and χ – T curves for site 1 and site 2 samples are shown in Figure 4 *a–d*. For site-1 samples, <95% of saturation is achieved at 200–300 mT, indicating a predominantly low-coercivity mineral contribution. This is supported by H_{cr} values ranging from 30 to 40 mT. The susceptibility drop at 580°C indicates magnetite as the remanence carrier in the sediments (Figure 4 *c*). IRM curves for site-2 samples show low-coercivity mineral contribution at 200–300 mT and H_{cr} values ranging from 30 to 50 mT. Thermomagnetic

(χ - T curve) experiments confirm that the two drops in susceptibility at 300°C and 580°C indicate the occurrence of titanomagnetite and magnetite respectively (Figure 4c).

From this study it can be concluded that the undeformed sediments are characterized by sedimentary oblate AMS ellipsoids, whereas the deformed sediments are characterized by distinct triaxial AMS ellipsoids. The site mean ChRM direction for deformed sediments is much more scattered with a precision parameter (k) 39 as opposed to 92.7 for undeformed sediments. The study also reveals simple analysis of the orientations of the K_3 axes; which shows that disturbed intervals are actually more tightly grouped and more vertical than the undisturbed intervals. This shows that sediments can be severely deformed without deflecting K_3 , but with a scattered ChRM direction. This may have a bearing on palaeomagnetic studies, though our results indicate that remanent magnetization is locally affected by sediment deformation.

1. Sims, J. D., Earthquake-induced structures in sediments of the Van Norman Lake, San Fernando, California. *Science*, 1973, **182**, 161–163.
2. Sims, J. D., Determining earthquake recurrence intervals from deformational structures in young lacustrine sediments. *Tectonophysics*, 1975, **29**, 141–152.
3. Sieh, K. E., Prehistoric large earthquakes produced by slip on the San Andreas Fault at Pallet Creek, California. *J. Geophys. Res.*, 1978, **83**, 3907–3939.
4. Scott, P. and Price, S., Earthquake induced structures in young sediments. *Tectonophysics*, 1988, **147**, 165–170.
5. Ringrose, P. S., Paleoseismic (?) liquefaction event in late Quaternary lake sediment at Glen Roy, Scotland. *Terra Nova*, 1989, **1**, 57–62.
6. McCalpin, J. C. (ed.), Field techniques in paleoseismology. In *Paleoseismology*, Academic Press, London, 1996, p. 588.
7. Obermeier, S. F. et al., Evidence of strong earthquake shaking in the lower Wabash Valley from prehistoric liquefaction features. *Science*, 1991, **251**, 1061–1063.
8. Mohindra, R. and Bagati, T. N., Seismically induced soft sediment deformation structures (seismites) around Sumdo in Lower Spiti valleys (Tethys Himalayas). *Sediment. Geol.*, 1996, **101**, 69–83.
9. Mohindra, R. and Thakur, V. C., Historic large earthquake-induced soft sediment deformation features in the Sub-Himalayan Doon valley. *Geol. Mag.*, 1998, **135**(2), 269–281.
10. Rajendran, C. P. and Rajendran, K., Geological investigation at Killari and Ther, Central India and implications for paleoseismicity in the shield region. *Tectonophysics*, 1999, **308**, 67–78.
11. Sukhija, B. S. et al., Paleoliquefaction evidence and periodicity of large prehistoric earthquakes in Shillong Plateau, India. *Earth Planet. Sci. Lett.*, 1999, **167**, 269–282.
12. Upadhyay, R., Earthquake-induced soft-sediment deformation in the lower Shyok river valley, northern Ladakh, India. *J. Asian Earth Sci.*, 2003, **21**, 413–421.
13. Kotlia, B. S. and Rawat, K. S., Soft sediment deformation structures in the Garbyang palaeolake: evidence for the past shaking events in the Kumaun Tethys Himalaya. *Curr. Sci.*, 2004, **87**(3), 377–379.
14. Singh, S. and Jain, A. K., Liquefaction and fluidization of lacustrine deposits from Lahaul-Spiti and Ladakh Himalaya: geological evidences of paleoseismicity along active fault zone. *Sediment. Geol.*, 2007, **196**, 47–57.
15. Sukhija, B. S., Lakshmi, B. V., Rao, M. N., Reddy, D. V., Naga-bhushanam, P., Hussain, S. and Gupta, H. K., Widespread geologic evidence of a large Paleoseismic event near the meizoseismal area of the 1993 Latur Earthquake, Deccan Shield, India. *J. Indian Geophys. Union*, 2006, **10**(1), 1–14.
16. Babar, M., Radhakrishna, C., Yadava, M. G. and Ghute, B., Quaternary geology and geomorphology of Terna river basin in West Central India. *Quaternary Sci. J.*, 2012, **61**(2), 156–167.
17. Rajendran, C. P., Deformational features in the river bluffs at Ther, Osmanabad district, Maharashtra: evidence for an ancient earthquake. *Curr. Sci.*, 1997, **72**, 750–755.
18. Crone, A. J., Machette, M. N. and Bowman, J. R., Geologic investigations of the 1988 Tennant Creek, Australia, earthquakes – implications for paleoseismicity in stable continental regions. *US Geol. Surv. Bull.*, 1992, **2032-A**, 51.
19. Machette, M. N., Crone, A. J. and Bowman, J. R., Geologic investigations of the 1986 Marryat Creek, Australia earthquake – implications for paleoseismicity in stable continental regions. *US Geol. Surv. Bull.*, 1993, **2032-B**, 29.
20. Rajguru, S. N., Kale, V. S. and Badam, G. L., Quaternary fluvial systems in upland Maharashtra. *Curr. Sci.*, 1993, **64**, 817–822.
21. Jelinek, V., Statistical processing of anisotropy of magnetic susceptibility measured on groups of specimens. *Stud. Geophys. Geod.*, 1978, **22**, 50–62.
22. Kirschvink, J. L., The least squares line and plane and the analysis of paleomagnetic data. *Geophys. J. R. Astron. Soc.*, 1980, **62**, 699–718.
23. Tauxe, L., *Paleomagnetic Principles and Practice*, Kluwer, Boston, Massachusetts, 1998.
24. Tarling, D. H. and Hrouda, F., *The Magnetic Anisotropy of Rocks*, Chapman and Hall, London, 1993, p. 217.
25. Liu, B., Saito, Y., Yamazaki, T., Abdeldayem, A., Oda, H., Hori, K. and Zhao, Q., Paleocurrent analysis for the late Pleistocene–Holocene incised-valley fill of Yangtze delta, China by using anisotropy of magnetic susceptibility data. *Mar. Geol.*, 2001, **176**, 175–189.
26. Schwehr, K. and Tauxe, L., Characterization of soft-sediment deformation: detection of cryptoslumps using magnetic methods. *Geology*, 2003, **31**, 203–206.
27. Rosenbaum, J., Reynolds, R., Smoot, J. and Meyer, R., Anisotropy of magnetic susceptibility as a tool for recognizing core deformation: reevaluation of the paleomagnetic record of Pleistocene sediments from drill hole OL-92, Owens Lake, California. *Earth Planet. Sci. Lett.*, 2000, **178**, 415–424.
28. Crimes, T. P. and Oldershaw, M. A., Palaeocurrent determinations by magnetic fabric measurements on the Cambrian rocks of Saint Tudwal's Peninsula, North Wales. *Geol. J.*, 1967, **5**, 217–232.
29. Shor, A. N., Kent, D. V. and Flood, R. D., Contourite or turbidite?: Magnetic fabric of fine-grained Quaternary sediments, Nova Scotia continental rise. In *Fine-Grained Sediments: Deep Water Processes and Facies* (eds Stowe, D. and Piper, D.), Blackwell Scientific Publications, Oxford, 1984, pp. 257–273.
30. Jackson, M., Borradaile, G. J., Hudleston, P. J. and Banerjee, S. K., Experimental deformation of synthetic magnetite-bearing calcite sandstones: effects on remanence, bulk magnetic properties, and magnetic anisotropy. *J. Geophys. Res.*, 1993, **98**, 383–401.
31. Cronin, M., Tauxe, L., Constable, C., Selkin, P. and Pick, T., Noise in the quiet zone. *Earth Planet. Sci. Lett.*, 2001, **190**, 13–30.

ACKNOWLEDGEMENTS. We thank the Director, Indian Institute of Geomagnetism, Navi Mumbai for permission to publish this paper. We also thank the anonymous reviewer for valuable and constructive suggestions. B.V.L. thanks the Department of Science and Technology, New Delhi for financial assistance (No. SR/WOS-A/ES-15/2010).

Received 16 May 2014; revised accepted 13 October 2014